Journal of Controlled Release 358 (2023) 498–509

Contents lists available at ScienceDirect

Journal of Controlled Release

journal homepage: www.elsevier.com/locate/jconrel

Focused ultrasound enhances transgene expression of intranasal hGDNF DNA nanoparticles in the sonicated brain regions

Amirah E.-E. Aly [a,1], Tao Sun [c], Yongzhi Zhang [c], Zejun Li [a], Margee Kyada [a], Qingxi Ma [a], Linas Padegimas [b,2], Ozge Sesenoglu-Laird [b], Mark J. Cooper [b], Nathan J. McDannold [c], Barbara L. Waszczak [a,*]

[a] Department of Pharmaceutical Sciences, Northeastern University, Boston, MA, USA
[b] Copernicus Therapeutics, Inc., Cleveland, OH, USA
[c] Focused Ultrasound Laboratory, Department of Radiology, Brigham and Women's Hospital, Harvard Medical School, Boston, MA, USA

A B S T R A C T

The therapeutic potential of many gene therapies is limited by their inability to cross the blood brain barrier (BBB). While intranasal administration of plasmid DNA nanoparticles (NPs) offers a non-invasive approach to bypass the BBB, it is not targeted to disease-relevant brain regions. Here, our goal was to determine whether focused ultrasound (FUS) can enrich intranasal delivery of our plasmid DNA NPs to target deeper brain regions, in this case the regions most affected in Parkinson's disease.

Combining FUS with intranasal administration resulted in enhanced delivery of DNA NPs to the rodent brain, by recruitment and transfection of microglia. FUS increased transgene expression by over 3-fold after intranasal administration compared to intravenous administration. Additionally, FUS with intranasal delivery increased transgene expression in the sonicated hemisphere by over 80%, altered cellular transfection patterns at the sonication sites, and improved penetration of plasmid NPs into the brain parenchyma (with a 1-fold and 3-fold increase in proximity of transgene expression to neurons in the forebrain and midbrain respectively, and a 40% increase in proximity of transgene expression to dopaminergic neurons in the substantia nigra). These results provide evidence in support of using FUS to improve transgene expression after intranasal delivery of non-viral gene therapies.

1. Introduction

One of the biggest impediments to the development of disease-modifying therapeutics for neurodegenerative disorders, such as Parkinson's disease (PD), is the inability of macromolecules to cross the blood-brain barrier (BBB). Glial cell-line derived neurotrophic factor (GDNF) has demonstrated neuroprotective potential in several animal models of PD, however human clinical trials have failed to meet their primary endpoints. Previous neurotrophic factor-based therapies for PD attempted to circumvent the BBB by direct intracerebral injection or by intravenous injection of vectors that bypass the BBB [1–8]. However, the former methods are invasive, and the latter are non-targeted. An alternative method, intranasal delivery, is non-invasive and allows large therapeutics to circumvent the BBB while avoiding peripheral exposure. Administered therapeutics follow the trajectory of the olfactory and trigeminal nerve terminals to reach the CNS, where they mix with CSF and travel throughout the brain in perivascular spaces [9].

We have recently investigated intranasal administration of unimolecularly compacted DNA nanoparticles (NPs) comprised of 10 kDa polyethylene glycol-substituted lysine 30-mer peptides (CK30PEG10k) and plasmid DNA [10,11] expressing human GDNF under the control of the polyubiquitin C (UbC) promoter, which provides long-term expression of GDNF in the brain regions associated with PD [12]. When administered intranasally, these hGDNF plasmid DNA NPs (pGDNF_1b NPs) were neuroprotective in the unilateral rat 6-OHDA model, successfully conserving dopaminergic fiber density and cell counts in the lesioned substantia nigra, and nerve terminal density in the lesioned striatum [13]. Furthermore, we have utilized a modified pGDNF_1b reporter plasmid, encoding eGFP linked to hGDNF (named pUGG), which is also transcriptionally controlled by the UbC promoter. We demonstrated that the intranasal administration of pUGG NPs results in widespread transfection of perivascular cells in the brain, and this

* Corresponding author at: Northeastern University, Room 269, 140 The Fenway, 360 Huntington Avenue, Boston, MA, USA.
E-mail address: b.waszczak@northeastern.edu (B.L. Waszczak).
[1] Centre for Molecular Medicine and Therapeutics, British Columbia Children's Hospital Research Institute, University of British Columbia, Vancouver, British Columbia, Canada.
[2] Abeona Therapeutics, Inc., Cleveland, Ohio, USA.

https://doi.org/10.1016/j.jconrel.2023.04.041
Received 6 January 2023; Received in revised form 20 April 2023; Accepted 26 April 2023
Available online 15 May 2023

expression lasts for at least 6 months [14].

While intranasal delivery successfully bypasses the BBB and minimizes systemic exposure, delivery within the brain is not targeted to specific regions, which may be a limitation when targeting is desired. A non-invasive approach to open the BBB and permit spatial targeting is focused ultrasound (FUS) with intravascular microbubbles. The application of FUS has been utilized in many studies to transiently improve the permeability of the BBB, in order to allow or enhance delivery of therapeutic agents to brain regions of interest. Combining ultrasound with circulating microbubbles can temporarily disrupt components of the BBB without apparent neuronal damage or lesions [15,16]. With MRI or stereotaxic guidance, it is possible to focus pulsed sonications to specific brain areas in order to disrupt the BBB in a localized region with little effect on the surrounding parenchyma. Most FUS studies carried out on small animals showed that BBB function was restored within a few hours of sonication [17–19].

Although FUS does improve brain permeability of therapeutic and diagnostic agents administered intravenously [20–23], high systemic doses would still need to be given to achieve therapeutic concentrations in the CNS target regions. This may result in off-target side effects or toxicity in the periphery. For an agent such as GDNF protein, systemic administration would cause high circulating levels and increase risk of peripheral side effects, since the receptors involved in GDNF signaling, GFRα and RET, are found in a number of peripheral tissues [24]. These concerns could override potential benefits of getting it into the brain and limit its therapeutic usefulness. For this reason, we and others have reasoned that combining FUS with intranasal delivery may exploit the advantages and minimize the disadvantages of both techniques, i.e., providing a completely non-invasive avenue for drug delivery to the CNS that is both substantial and targeted whilst minimizing systemic exposure to the therapeutic agent [25–27].

Here, we explore whether combining FUS with intranasal delivery could provide a means of increasing CNS bioavailability, tissue penetration, and/or regional delivery of our hGDNF NPs. If successful, this gene therapy approach might overcome the main limitations of intranasal drug delivery, i.e., low efficiency, due to the fact that only a fraction of the administered doses reaches the brain, and untargeted CNS delivery, due to the fact that the entire brain is exposed to the agent. Combining FUS with intranasal administration of a therapeutic gene vector may both improve delivery to the targeted regions and increase transgene expression at target sites. For Parkinson's disease, in particular, this approach may result in greater overall delivery of hGDNF NPs to areas affected, the substantia nigra (SN) and striatum, with improved tissue penetration and enrichment of transgene expression at these sites of neural degeneration.

2. Materials and methods

2.1. pUGG plasmid construction

The plasmid used in these studies was derived from the hGDNF plasmid splice variant 1 pGDNF_1b, reported in Fletcher et al. [12] The eGFP-GDNF plasmid, termed pUGG, was created by removing the signal sequence from the pGDNF_1b plasmid construct and inserting the cDNA for eGFP in its place (Sup Fig. 1).

2.2. Formulation of compacted DNA nanoparticles

Compacted DNA NPs were formulated by slowly adding 20 ml of DNA solution (0.1 mg/ml) to a mixing solution of 2.0 ml (3.2 mg/ml) of CK30PEG10k (American Peptide Company, Sunnyvale, CA) with an acetate counterion [10,11,28,29]. Compacted DNA was filtered through a sterile 0.2 μm polyethersulfone membrane and then processed with tangential flow filtration in exchange with saline. Further concentration steps were performed using VIVASPIN centrifugal concentrators (MWCO 100 k).

2.3. Animal treatments

Studies were carried out in naïve male Sprague-Dawley (SD) rats weighing 200–250 g (Taconic) in strict compliance with protocols approved by both the Northeastern University IACUC and Harvard Medical School IACUC.

For intranasal treatments, rats were anesthetized with ketamine and xylazine (90/20 mg/kg, i.p.) and then placed in a supine position with their noses upright and heads flat on the surface. A 10 μl Hamilton syringe with a 1.5 cm piece of polyethylene tubing fitted on the needle tip was used to administer either pUGG NPs or saline in 2.5 μl increments per nare every 2 min alternating sides until the total volume (18 μl) was given. The total dose of pUGG DNA was 93 μg. Rats remained supine for 30 min after intranasal administration.

For intravenous treatments, the animals received the same dose of pUGG NPs (93 μg DNA) via tail vein catheter, in a volume of 140 μl 0.9% NaCl.

This dose (93 μg DNA) was chosen based on our previously published works demonstrating that intranasal doses of our DNA NPs ranging from around 86–96 μg DNA resulted in significant increases in transgene expression throughout the brain [13,14,28].

2.4. Focused ultrasound with circulating microbubbles

A dual-aperture FUS setup was used (f = 274.3 kHz), and a passive detector ($f_{central}$ = 650 kHz) monitored cavitation activity during FUS treatments. Detailed acoustic design and performance demonstration were reported previously [30]; in summary the axial dimension was FWHM 6.4 mm, for measurements, and the transverse dimensions were FWHM: 9.7 × 6.5 mm. FUS bursts (32 msec bursts at 4 Hz for 100 s) were applied during infusion of Optison microbubbles (200 μl/kg) to a dorsal brain region in the right hemisphere before intranasal delivery and repeated 1 h later with microbubbles at a caudal location on the same side after intranasal delivery. For rats that received intravenous (IV) treatments via tail vein catheter, the second set of FUS bursts was repeated 10 min after IV administration of pUGG NPs. The peak negative pressure amplitude during sonication was feed-back controlled as described previously [31] with a maximum level of 616 kPa. Total amount of stable cavitation (harmonic emissions) was delivered at 12×10^3dB for each targeted area.

An acoustic emissions-based controlling paradigm that can sustain stable cavitation (harmonic emission, HE) while suppressing inertial cavitation (broadband emission, BE) was used. HE and BE were analyzed during 32-ms bursts in real time and fed back for control of the next pulse. To avoid inertial cavitation, the pressure was reduced if BE was detected and terminated if it crossed a set threshold, i.e., sonication would be halted if a preset integrated HE goal (30 dB) was achieved. This FUS controlling system has been demonstrated to sustain stable cavitation behavior while suppressing the inertial cavitation at a minimum level. This real-time closed-loop controller enables the reliable delivery of a pre-determined amount of drug to the brain [31].

Safety profiles of this sonication system were characterized in our previous published studies [30,31]. Our work and others [32] confirmed that there is an effective (and quasi-linear) cavitation window under this frequency range for BBB opening, and that our cavitation based controller is able to monitor and modulate the drug delivery. We have previously demonstrated [31] with H&E staining that our BBB-opening system with these parameters results in no vascular, ischemic or neuronal damage in the sonicated targets or surrounding regions.

2.5. Preparation of brain tissue

For immunohistochemistry, the animals were sacrificed by transcardial perfusion under isoflurane anesthesia with phosphate-buffered saline (PBS) followed by 4% paraformaldehyde (PFA) in PBS. Brains were removed and post-fixed in 4% PFA for 24 h and then placed in 30%

sucrose for 2–4 days. The brains were then cryo-sectioned at 25 μm and sections were stored at −20 °C in a cryoprotectant solution (30% sucrose, 0.01% polyvinylpyrrolidone-40, 30% ethylene glycol, 50% PBS, in distilled H_2O).

For brains processed by ELISA, rats were sacrificed by decapitation under isoflurane anesthesia. Brains were rapidly removed, weighed, and transferred to an acrylic rat brain matrix with 1 mm coronal slice intervals. Coronal sections (approximately 3 mm thick) were cut, flash frozen in liquid nitrogen, and then stored at −80 °C. Each section was homogenized in 1 ml of lysis buffer (1% Igepal, 0.1% Triton-x, 10% glycerol, and 1:100 protease inhibitor in PBS) using a 1 ml dounce homogenizer. Homogenates were centrifuged at 14,000 RPM for 30 min at 4 °C, and the supernatants were stored at −80 °C for later analysis by ELISA.

2.6. Double-label immunohistochemistry for detection of eGFP with RECA-1, GFAP, NeuN, or Iba1

Free-floating coronal sections of rat brain (25 μm thick) were blocked in a solution containing 10% normal goat serum (NGS) and 10% normal donkey serum (NDS) in PBS for 1 h. Sections were then incubated overnight at 4° C with primary antibodies to both eGFP (rabbit anti-GFP; Ab290 from Abcam; 1:2000) and either rat endothelial cell antigen-1 (RECA-1; mouse anti-RECA-1; Abcam AB9774; 1:1000), GFAP (mouse anti-GFAP, Millipore MAB360; 1:1000), NeuN (mouse anti-NeuN; Millipore MAB377; 1:1000), or ionized calcium-binding adapter molecule 1 (Iba1; goat anti-Iba1, Abcam AB107159; 1:1000) in PBS containing 5% NDS and 5% NGS. Sections were then incubated for 1 h with the corresponding secondary antibodies diluted 1:2000 in PBS. The secondary antibodies were donkey anti-rabbit IgG conjugated to Alexa Fluor® 647 (Ab150075, Abcam) for detection of eGFP, goat anti-mouse IgG conjugated to Alex Fluor® 488 (Ab150117, Abcam) for detection of GFAP, RECA-1, NeuN, or donkey anti-goat IgG conjugated to Alexa Fluor® 488 (AB150133) for detection of Iba1. Sections were mounted on slides and coverslipped using Fluoromount-G (Southern Biotech).

2.7. Detection of eGFP by ELISA

ELISAs were carried out in 96-well plates; a final volume of 100 μl/well was maintained throughout assays. The wells were coated with GFP capture antibody in a 1:4000 dilution in PBS (mouse anti-GFP, Sigma #G-6539) and incubated at 4 °C overnight. All subsequent steps were carried out at room temperature with continuous shaking. Between steps, plates were washed three times with wash buffer (0.05% Tween-20 in PBS). Plates were blocked using 100 μl/well of 5% non-fat dry milk in PBS for 1 h. The eGFP standards were serially diluted (from 1000 pg/ml to 7.81 pg/ml) in reagent diluent (1% BSA in PBS). Reagent diluent was used for blanks. Samples and blanks were added, and plates were incubated at room temperature for 2 h. Next, the eGFP detection antibody (rabbit anti-GFP; Abcam, AB290; 1:4000 dilution in reagent diluent) was added to the wells and incubated for 1.75 h. The secondary antibody, anti-rabbit conjugated to HRP (GE #NIF824) diluted 1:4000 in reagent diluent, was then added and the plates were incubated for 45 min. SureBlue TMB substrate (KPL #52–00-01) was added to the wells and incubated for 10–15 min until full colour development occurred. The reaction was stopped by addition of 100 μl 1 N HCl to each well.

2.8. Microscopy

Microscopic analyses were performed using an Olympus BX51 microscope equipped with X-cite fluorescence and DIC optics for contrast enhancement, and images were captured by a QImaging camera. Fluorescence microscopy for detection of eGFP and a second cellular marker (RECA-1, GFAP, NeuN, Iba1) was carried out using red and green excitation/emission filter sets.

2.9. Bioquant analysis

eGFP-positive cells (stained with Alexa Fluor 647) were observed microscopically and quantified using Bioquant Nova version 6.90.1 image analysis software. A conditional frequency analysis was conducted using Bioquant to determine the proportion of eGFP-positive cells in each field that overlapped a second cellular marker indicating either RECA-1, GFAP, NeuN, or Iba1 (stained with Alexa fluor 488). Counting fields were randomly selected using Bioquant's random grid generator superimposed over the areas of interest. The conditional frequency analysis was done by first examining the tissue section at 40× using the red fluorescence filter to locate all cells that appeared to contain eGFP. The eGFP-positive (red) cells were then identified with circles on the Bioquant image, and the total number was recorded. Then the same field was viewed using the green filter (without moving the section or adjusting focus), and the number of green cells that co-localized with the red cells circled using the red filter was counted. Results were expressed as the percentage of eGFP-positive (red) cells that co-registered with (green) cells positive for the second cellular marker. The conditional frequency analysis of double labeling was done for at least 3 sections from each brain region of each rat from the different treatment groups. All cell counting was performed by a person blinded to intranasal treatments.

2.10. Statistical analyses

A power analysis was carried out to determine sample sizes for studies involving whole brain eGFP ELISAs. Estimated mean differences between groups were based on previously reported data [28]. It was determined that 6 rats per group would achieve 95% power (β) for a two-sided *t*-test comparing means of two independent samples, assuming unequal variances and $\alpha = 0.05$.

Statistical analyses were performed using GraphPad Prism® software version 4.03. The α-level for significance was set at 0.05. Values are presented as mean ± standard error of the mean (SEM). Comparisons between multiple groups were conducted by analysis of variance (ANOVA) with the appropriate post-hoc test to determine the significance of differences between groups. Comparisons between two groups of data were performed using Student's *t*-test.

3. Results

3.1. FUS spatially shifted the distribution of intranasal pUGG NP transgene expression to the sonicated hemisphere

Our first goal was to examine transgene expression in rat brain after combining microbubble-mediated FUS and intranasal delivery of pUGG NPs. Naïve rats ($n = 7$) were subjected to FUS with circulating microbubbles before and after intranasal administration of pUGG NPs (93 μg DNA). The first FUS treatment was applied to a rostral brain region (at the level of the striatum, brain regions A and B; Sup Fig. 2) in the right hemisphere beginning 10 min before intranasal delivery of pUGG NPs. The same FUS sequence was repeated 1 h later at a caudal location (at the level of the midbrain, brain region C; Sup Fig. 2) on the same side. Contrast-enhanced MRI following the FUS treatment confirmed the BBB disruption (Fig. 1c, d). Rats were sacrificed one week later, and brains were cut into 4 rostral-to-caudal coronal slabs (designated A-D), separating the left and right sides of each slab (designated L and R). Transgene expression throughout the brain was assessed by eGFP-ELISA.

Since FUS-mediated BBB opening is transient and is highest immediately following sonication and decreases as a function of time [16], and since the majority of intranasally delivered substances reach the most caudal brain regions within 1 h [9], we reasoned that extending the total length of BBB opening using two FUS treatments, one just before and one just after intranasal dosing, would allow sufficient overlap between the timeframe with highest BBB-opening for each sonication site

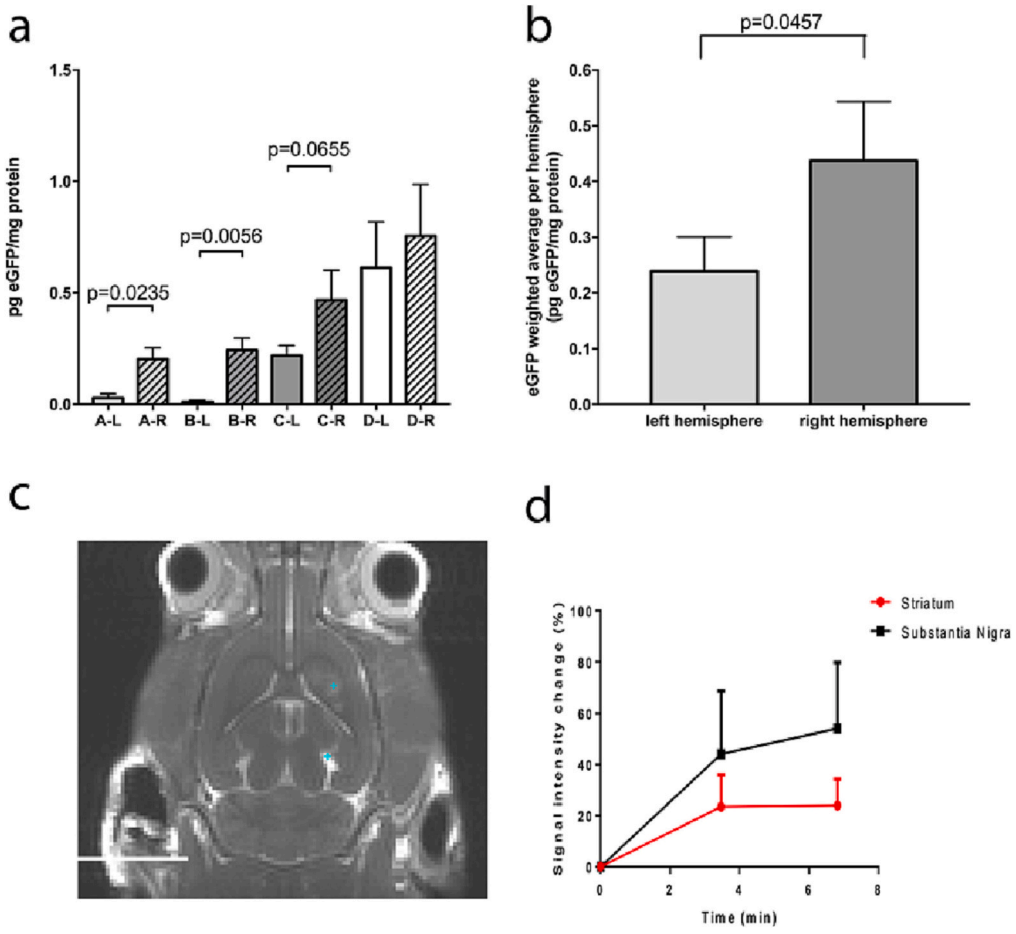

Fig. 1. Combining intranasal delivery of pUGG NPs with FUS shifts transgene expression to sonicated hemisphere. FUS with circulating microbubbles was applied before (to forebrain, B) and after (to the midbrain, C) intranasal administration of pUGG NPs (90 μg DNA) to rats (n = 7). (a) FUS resulted in increased eGFP expression in the three most rostral brain regions (A, B, and C) of the sonicated right (R) hemisphere relative to the unsonicated (L) brain regions. One-way ANOVA: P = 0.0004; paired t-test, L vs R for each region: A: P = 0.023, B: P = 0.0056, C: P = 0.0655. Rostral to caudal brain regions: A (olfactory bulbs and frontal cortex), B (forebrain), C (midbrain), D (cerebellum and pons/medulla). (b) FUS with microbubbles significantly increased the weighted average of eGFP expression in the sonicated right hemisphere vs the unsonicated left hemisphere. Paired t-test: P = 0.0457. (c) T1-weighted contrast MRI scan confirming BBB disruption (light spots marked with blue asterisk). (d) No statistical difference in contrast enhancement between forebrain (striatum) and midbrain (substantia nigra) sites was found, indicating comparable BBB disruptions in the two targeted areas.

and the period during which transport of intranasally delivered NPs in perivascular spaces is highest.

FUS with circulating microbubbles increased eGFP expression in the three most rostral brain regions (A, B, and C) of the sonicated right hemisphere, relative to the unsonicated left brain regions, by over 7-, 24-, and 2-fold respectively. (Fig. 1a; one-way ANOVA indicated significance by treatment; individual paired t-tests, L vs R for A: P = 0.023, B: P = 0.0056, C: P = 0.0655). This translated to a significant increase (by about 83%) in the weighted average of eGFP expression in the sonicated right hemisphere of rats given intranasal pUGG NPs with FUS compared to the unsonicated left hemisphere. (Fig. 1b; individual paired t-test: P = 0.0457). Although eGFP expression was highest in the most caudal section, D, in agreement with our previous studies which showed the highest distribution of nasally administered substances to the most caudal brain areas [14,28,33], there was no significant left-to-right difference at this level. Only the sonicated (right) side of sections A, B and C showed significant increases in eGFP expression relative to the left (control) side. Thus, FUS with circulating microbubbles, when combined with intranasal administration of pUGG NPs, resulted in higher transgene expression in the sonicated brain regions and increased total transgene expression on the sonicated side of the brain.

3.2. FUS increased pUGG NP transgene expression to a greater extent after intranasal than intravenous administration of the same dose

Our next goal was to evaluate whether FUS with circulating microbubbles enhanced to a greater extent intravenous versus intranasal delivery of the same dose of pUGG NPs to the brain and to assess the relative regional distribution of that transgene expression in rat brain. The same study design was used as above, with minor modifications. Rats (n = 7) underwent sonication (32 msec bursts at 4 Hz for up to 100 s) at a forebrain region in the right hemisphere (area B), then received the same dose of pUGG NPs (93 μg DNA) intravenously in a volume of 140 μl 0.9% NaCl. They were then subjected to a second sonication using the same FUS sequence ten minutes later at a more caudal location (area C) on the same side. Contrast-enhanced MRI following the FUS treatment confirmed the BBB disruption at both sites (Fig. 2d, e).

In rats given intravenous pUGG NPs, FUS with circulating microbubbles resulted in significantly less whole brain eGFP expression (about a 3.6-fold lower expression) than was observed with intranasal pUGG NPs with or without FUS treatment. (Fig. 2a; one-way ANOVA indicated significance by treatment: [F(2,11) = 1.315, P = 0.0253]; Holm-Sidaks' multiple comparisons test: IN pUGG vs IN pUGG NP + FUS: P = 0.9483, n.s.; IN pUGG vs IV pUGG + FUS: P < 0.05; IN pUGG + FUS vs IV pUGG + FUS: P < 0.05). Furthermore, after intravenous administration of pUGG NPs, FUS did not increase whole brain eGFP expression relative to controls given intranasal saline. eGFP expression in the sonicated (right) brain regions (A through C) and the sonicated (right) hemisphere were not significantly increased compared to the unsonicated (left) controls (Fig. 2b,c). One-way ANOVA by region (Fig. 2b) indicated significance by treatment: [F(7,48) = 3.533, P = 0.0039] but individual paired t-tests showed significance only for D-L vs D-R, P = 0.0022. A paired t-test indicated no significance differences by hemisphere (Fig. 2c; L versus R hemisphere: P = 0.0658, n.s.).

These data show that intranasal delivery is much more effective in leading to transgene expression in the rat brain than intravenous administration of the same dose, and that FUS with microbubbles does not appreciably improve that outcome for intravenously administered pUGG NPs despite the modest hemispheric difference.

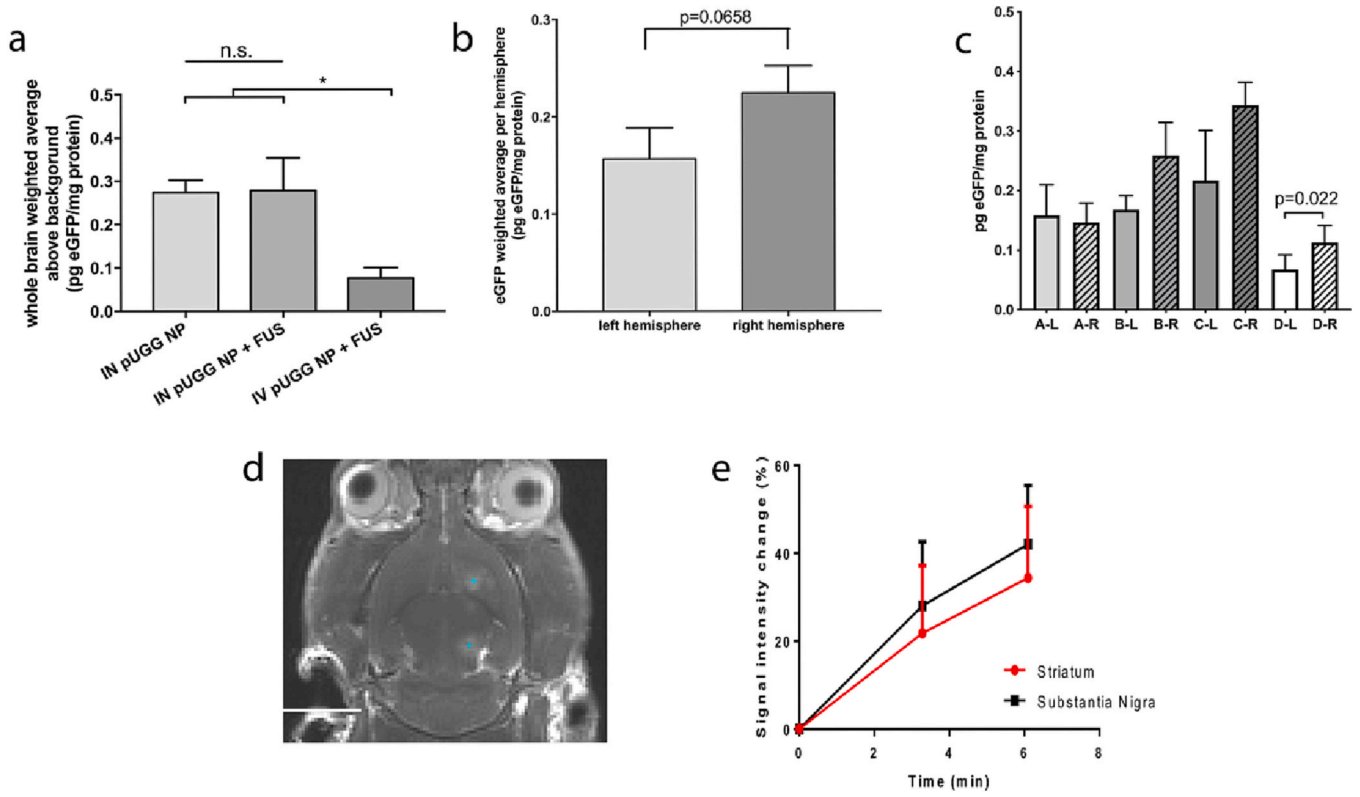

Fig. 2. Combining intravenous delivery of pUGG NPs with FUS does not result in a global or hemispheric difference in transgene expression. FUS with circulating microbubbles was applied before (to forebrain, B) and after (to the midbrain, C) intranasal or intravenous administration of pUGG NPs (90 μg DNA) to rats ($n = 7$/group). (a) In rats given intravenous pUGG NPs, FUS with microbubbles did *not* increase whole brain weighted average eGFP expression compared to rats given intranasal pUGG NPs with or without FUS. One-way ANOVA of background corrected data, $P = 0.0253$, Holm-Sidak's multiple comparison test: $P < 0.05$. (b) FUS with microbubbles only slightly increased the weighted average of eGFP expression in the sonicated versus unsonicated hemisphere of the brain after IV pUGG NP treatment. Paired *t*-test: $P = 0.0658$. (c) In rats given IV pUGG NPs, FUS with microbubbles did *not* increase eGFP expression on the right vs left side, except for the most caudal section, D. One-way ANOVA, $P = 0.0039$; paired t-test, D-L vs D-R: $P = 0.0022$). (d) T1-weighted contrast MRI scan confirming BBB disruption (light spots marked with blue asterix). (e) No statistical difference in contrast enhancement between forebrain (striatum) and midbrain (substantia nigra) sites was found, indicating comparable BBB disruptions in the two targeted areas.

3.3. FUS altered cellular transfection patterns at the sonication site compared to intranasal delivery alone

Another goal of this study was to determine whether FUS with circulating microbubbles alters cellular transfection patterns in the brain as a result of intranasal administration of pUGG NPs. In previous studies [14], we showed that cells transfected by intranasal pUGG NPs were typically perivascular cells that were not astrocytes, neurons, or vascular endothelial cells. We speculated that these cells were pericytes. In animals that received intranasal pUGG NPs with FUS, the pattern of transfection in areas *not* at the sonication site was similar to that after intranasal delivery alone, as the majority of transfected cells were located immediately adjacent to and abluminal to blood vessels. However, here we show that these cells were often Iba1-positive (Sup Fig. 3), suggesting their identification as either pericytes, microglia, or perivascular macrophages, all of which have been known to express this immunohistochemical marker [34,35]. Alternatively, these Iba-1-positive perivascular cells might be pericytes that have become transfected by pUGG NPs and are in the process of differentiating into microglia. The conversion of pericytes into microglia is a possibility raised in recent reports [36,37].

On the other hand, at the sonication sites, which were identified by discrete clumps of more intense eGFP staining at the same location in multiple sections, a large number of eGFP-positive cells were observed that did not co-localize with RECA-1 (Fig. 3), GFAP (Fig. 4), or NeuN (Fig. 5). These dense clusters of larger amoeboid-shaped cells were not seen at non-sonicated sites. At the putative sonication sites, the discrete clumps of transfected cells extended deep into the parenchyma, and nearly all of these GFP-positive cells were also Iba1-positive (Fig. 6), identifying them as transfected microglia. In fact, 76% and 89% of GFP-positive cells at the forebrain and midbrain sonication sites, respectively, co-localized with Iba1, compared to only 26–39% in non-sonicated sites at the same level (Fig. 7). GFP-positive cells observed in normal, non-sonicated tissue may be pericytes or resting microglia considering their discrete ovoid or extended morphology along vessel walls (as shown in Sup Fig. 3). They did not resemble activated microglia. However, at sonication sites, the transfected Iba-1-positive cells were larger ameboid cells located in irregular clumps extending into the parenchyma, not aligned along vessel walls, and they appeared to be activated microglia (Fig. 6). The fact that transfected, Iba-1-positive cells at non-sonication sites did not have features of activated microglia suggests that pGDNF NPs did not cause microglial activation. Conversely, sonication by itself did appear to induce microglial activation (similar to what was observed in other studies [38,39]), and a sizable subpopulation also became transfected by pGDNF NPs.

To further assess whether FUS with circulating microbubbles was responsible for microglial activation/recruitment at the sonication site, control rats underwent FUS treatments (using the same sonication parameters) but with no intranasal NPs (i.e., they received intranasal saline instead). Results of Iba1-I IHC indicated that FUS with circulating microbubbles did indeed recruit microglia to sonication sites, even in the absence of DNA NPs. This was evidenced by dense clumps of ameboid, Iba-1-labeled cells at apparent sonication sites, which were distinct from the widely dispersed normal microglia at adjacent areas in

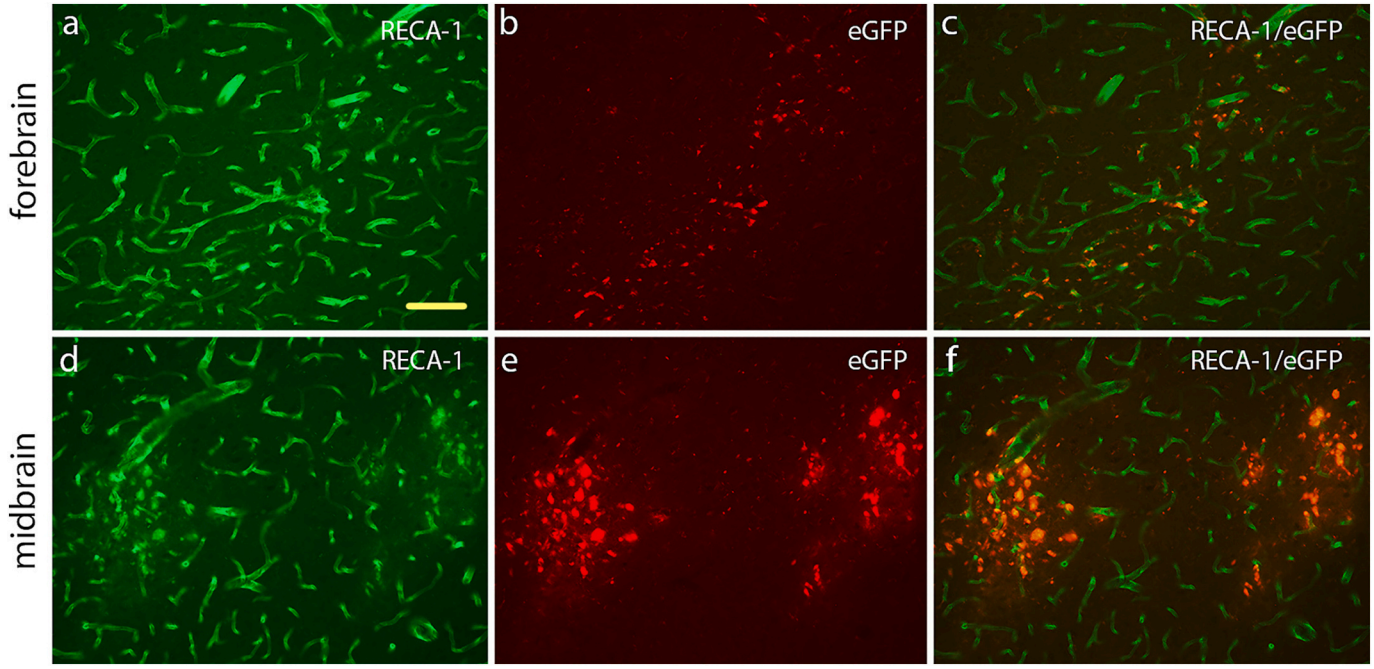

Fig. 3. Representative images of RECA-1 and eGFP stained sections from the sonication sites in rats that received intranasal pUGG NPs and FUS with circulating microbubbles. FUS with circulating microbubbles was applied before (to forebrain, a-c) and after (to the midbrain, d-f) intranasal administration of pUGG NPs (90 μg DNA) to rats (n = 4). Forebrain and midbrain sections underwent double-label IHC with markers for eGFP (red) and RECA-1 (green). The majority of eGFP transfected cells at the sonication sites in both the forebrain and midbrain did not appear to colocalize with RECA-I-positive cells. (Left panel) RECA-1 staining; (Middle panel) eGFP staining; (Right panel) Overlayed images of RECA-1 and eGFP staining. Scale bar = 80 μm

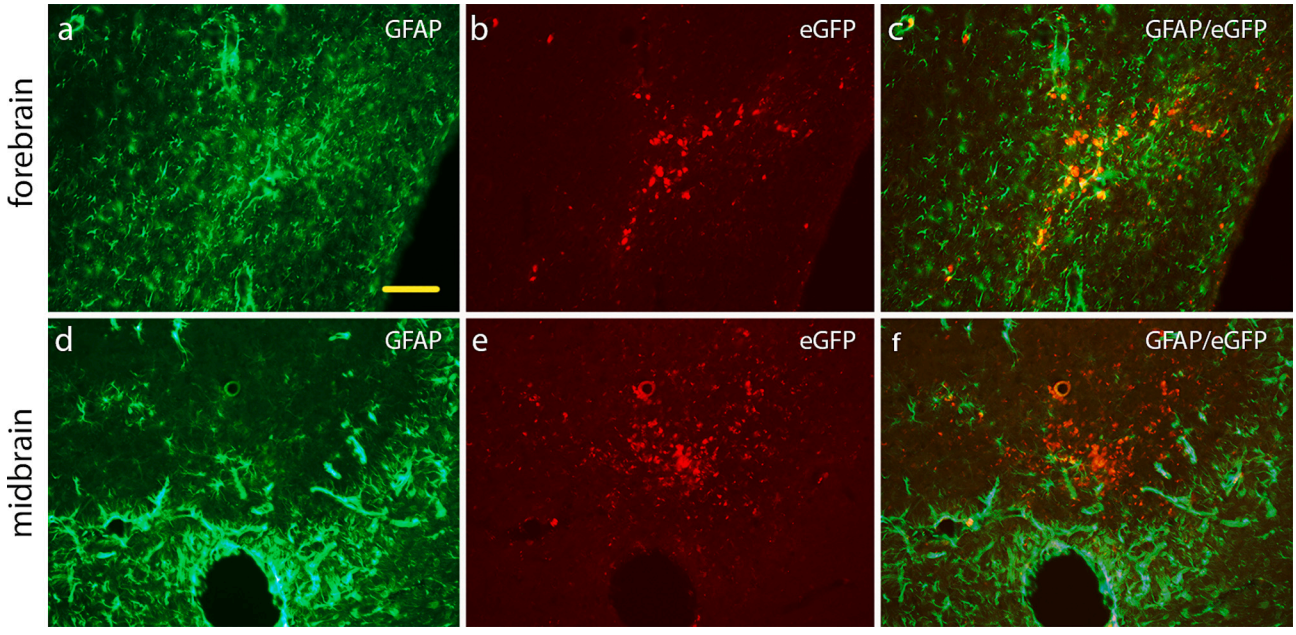

Fig. 4. Representative images of GFAP and eGFP stained sections from the sonication sites in rats that received intranasal pUGG NPs and FUS with circulating microbubbles. FUS with circulating microbubbles was applied before (to forebrain, a-c) and after (to the midbrain, d-f) intranasal administration of pUGG NPs (90 μg DNA) to rats (n = 4). Forebrain and midbrain sections underwent double-label IHC with markers for eGFP (red) and GFAP (green). The majority of eGFP transfected cells at the sonication sites in both the forebrain and midbrain did not appear to colocalize with GFAP-positive cells. (Left panel) GFAP staining; (Middle panel) eGFP staining; (Right panel) Overlayed images of GFAP and eGFP staining. Scale bar = 80 μm

the tissue (Fig. 8).

3.4. FUS increased the proximity of eGFP-positive cells to NeuN-positive cells and to TH-positive dopaminergic neurons in the midbrain

It was next of interest to determine if FUS with microbubbles changed the distribution and penetration of pUGG NPs into the brain

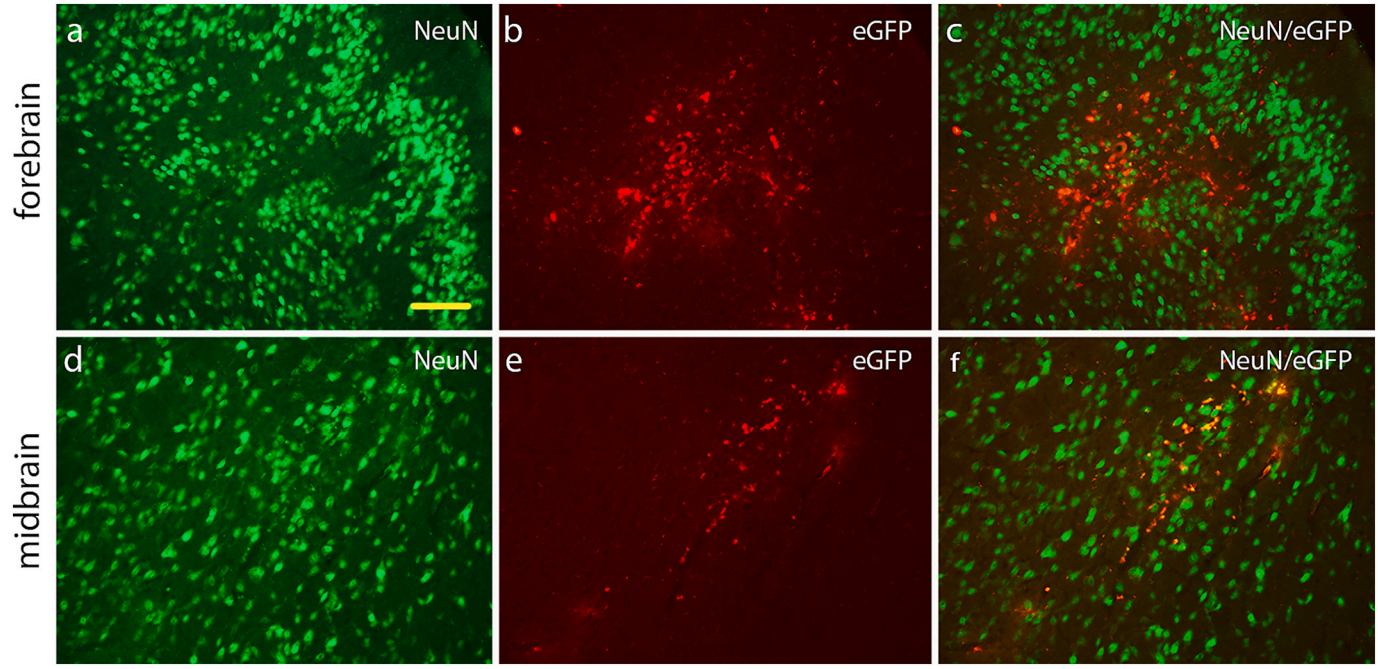

Fig. 5. Representative images of NeuN and eGFP stained sections from the sonication sites in rats that received intranasal pUGG NPs and FUS with circulating microbubbles. FUS with circulating microbubbles was applied before (to forebrain, a-c) and after (to the midbrain, d-f) intranasal administration of pUGG NPs (90 μg DNA) to rats ($n = 4$). Forebrain and midbrain sections underwent double-label IHC with markers for eGFP (red) and NeuN (green). The majority of eGFP transfected cells at the sonication sites in both the forebrain and midbrain did not appear to colocalize with NeuN-positive cells. (Left panel) NeuN staining; (Middle panel) eGFP staining; (Right panel) Overlayed images of NeuN and eGFP staining. Scale bar = 80 μm.

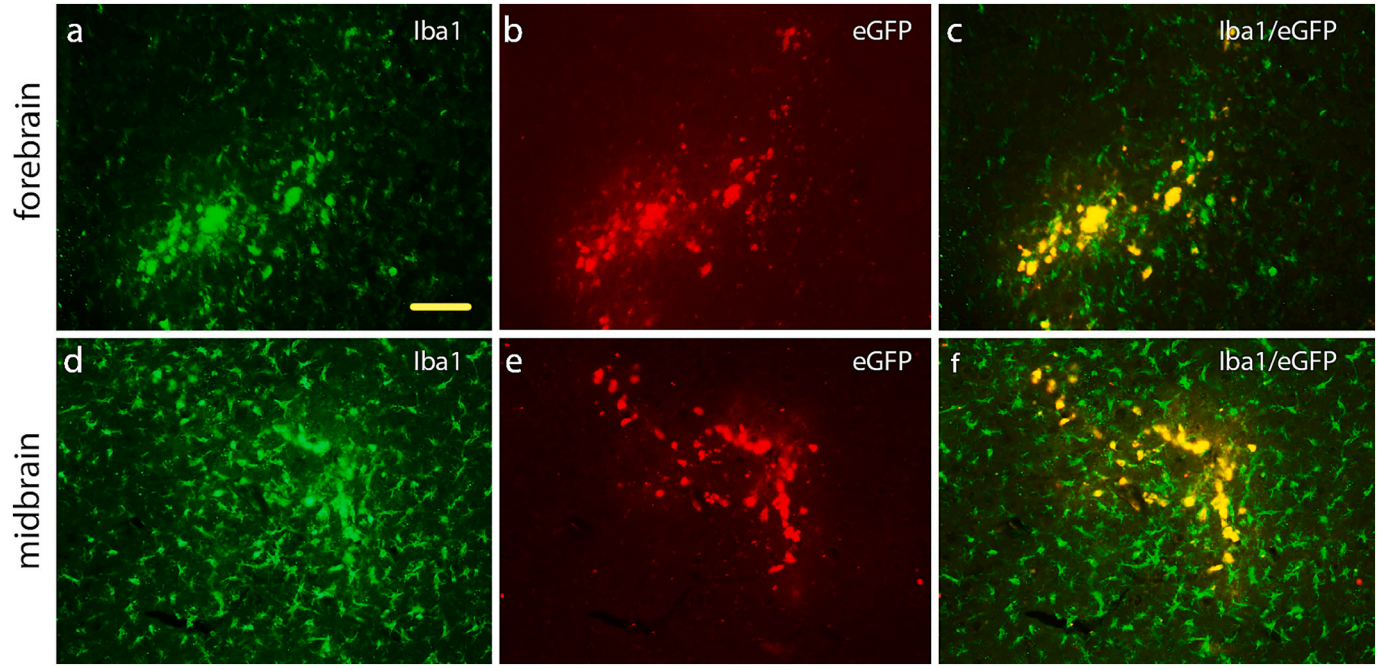

Fig. 6. Representative images of Iba1 and eGFP stained sections from the sonication sites in rats that received intranasal pUGG NPs and FUS with circulating microbubbles. FUS with circulating microbubbles was applied before (to forebrain, a-c) and after (to the midbrain, d-f) intranasal administration of pUGG NPs (90 μg DNA) to rats (n = 4). Forebrain and midbrain sections underwent double-label IHC with markers for eGFP (red) and Iba1 (green). The majority of transfected cells at the sonication sites in both the forebrain and midbrain colocalized with Iba1-postiive cells. (Left panel) Iba1 staining; (Middle panel) eGFP staining; (Right panel) Overlayed images of Iba1 and eGFP staining. Scale bar = 80 μm.

parenchyma. In previous studies [14], it was determined that the majority of eGFP-positive cells after intranasal administration of pUGG NPs were located immediately adjacent to and abluminal to blood vessels throughout the brain. This localization of transfected cells (and thus any secreted GDNF) was presumably in close-enough proximity to neurons in the striatum and substantia nigra to afford neuroprotection in the 6-OHDA rat model of Parkinson's disease. However, since our goal was to increase the delivery of DNA nanoparticles to the striatum and

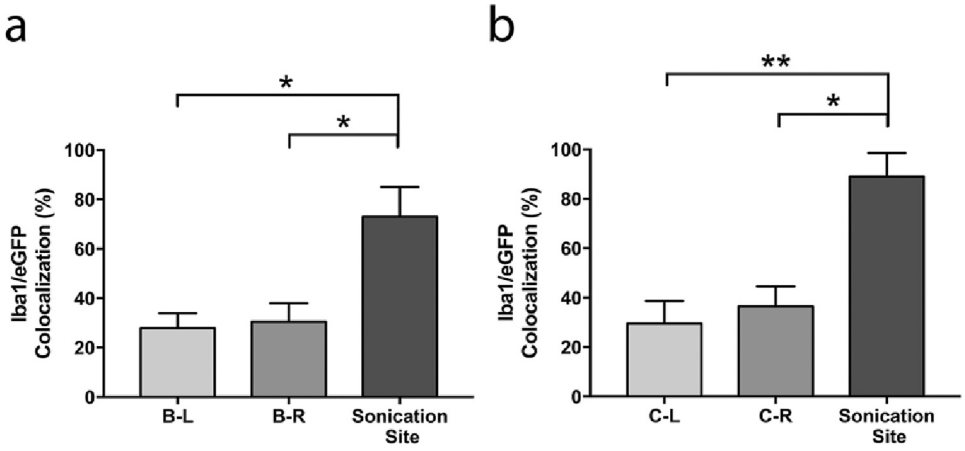

Fig. 7. FUS with microbubbles, when combined with intranasal delivery of pUGG NPs, results in significantly increased transfection of Iba1+ cells at the sonication sites in the forebrain (B), and midbrain (C) compared to non-sonicated sites at both regions. One-way ANOVA indicates significance by region ($P < 0.01$). Bonferroni post-tests indicate significantly higher colocalization at the sonication site compared to the left and right hemispheres of both forebrain (brain area B) and midbrain (brain area C) ($^*p < 0.05$, $^{**}p < 0.01$).

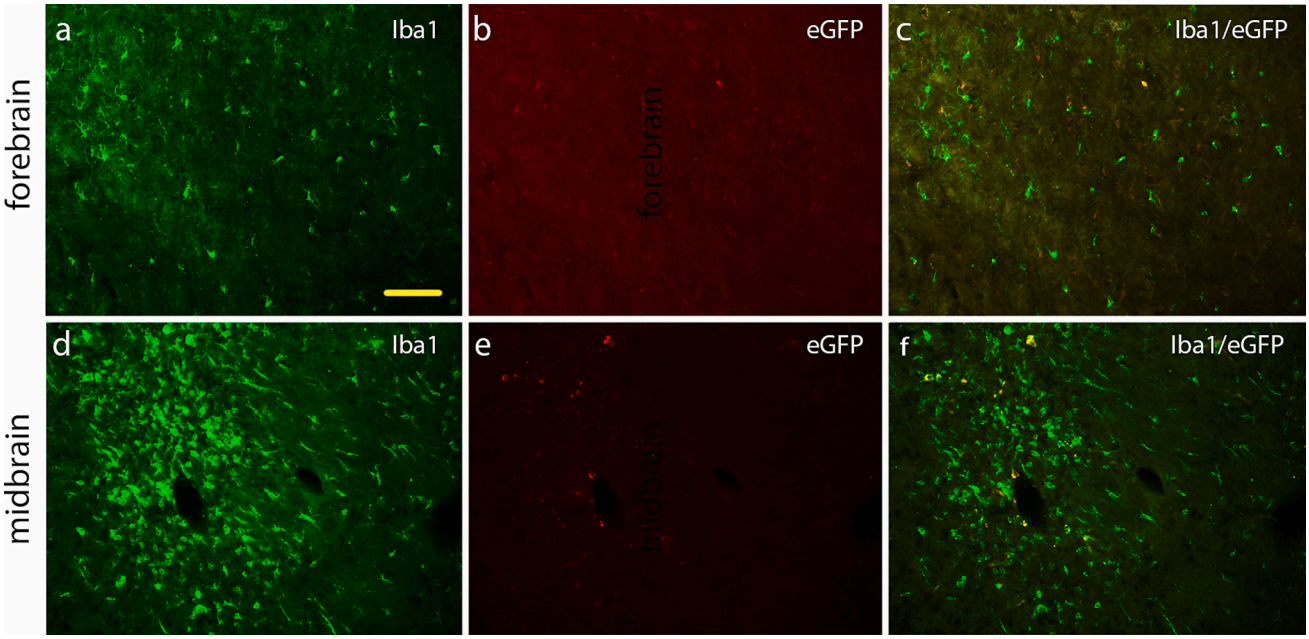

Fig. 8. Representative images of Iba1 and eGFP stained sections from the sonication sites in rats that received intranasal saline and FUS with circulating microbubbles. FUS with circulating microbubbles was applied before (to forebrain, a-c) and after (to the midbrain, d-f) intranasal administration of saline to rats ($n = 4$). Forebrain and midbrain sections underwent double-label IHC with markers for eGFP (red) and Iba1 (green). In the absence of intranasal DNA NPs, (i.e., no resulting eGFP expression), FUS with circulating microbubbles resulted in recruitment of Iba1-positive cells to the sonication sites in both the forebrain and midbrain. (Left panel) Iba1 staining; (Middle panel) eGFP staining; (Right panel) Overlayed images of Iba1 and eGFP staining. Scale bar = 80 μm.

substantia nigra as a gene therapy for Parkinson's disease, we next examined whether FUS altered the number of transfected cells that are closely adjacent to NeuN-positive cells or TH-positive neurons in these target brain regions. We used Bioquant to determine the percentage of transfected cells within 15 μm of these cell types. This distance, 15 μm, was chosen because the average distance from a neuron to the nearest microvessel in the brain is about 10–20 μm, ensuring optimal diffusion of nutrients, oxygen, and other molecules across the blood-brain barrier [40].

At sites distant from the sonication sites in the forebrain and midbrain of rats that received FUS with intranasal pUGG NPs, eGFP-positive cells remained in close proximity to RECA-1 positive capillary endothelial cells in the sonicated hemisphere. Correspondingly, the majority of eGFP-positive cells were also found within 15 μm of GFAP-positive astrocytes (Sup Fig. 4). This is consistent with our previous results [14] with animals that received the same dose of pUGG NPs intranasally without FUS. However, a significantly higher percentage of eGFP-positive cells were found within 15 μm of NeuN-positive cells in both the forebrain and midbrain regions of the sonicated rats, compared to animals that received intranasal pUGG NPs alone (Fig. 9a, b). For instance, in our previous colocalization study carried out after intranasal delivery of pUGG NPs alone (with no FUS), we found that 17% and 40% of eGFP-positive cells were in close proximity (within 15 μm) to a NeuN-positive neuron in the midbrain and forebrain, respectively [14]. In the animals that received intranasal pUGG NPs and underwent sonication in the striatum and midbrain, over 60% of eGFP-positive cells in both the sonicated and unsonicated hemispheres (distant from exact sonication sites) were located within 15 μm of a NeuN-positive neuron in both the forebrain and the midbrain (Fig. 9a, b). Thus, it appears that FUS also has subtle widespread effects, extending beyond discrete sonication sites, to increase tissue penetration of the NPs and enable transfection of cells deeper in the parenchyma. Similarly, in our previous colocalization study, approximately 60% of eGFP-positive cells were within 15 μm of TH-positive dopaminergic neurons in the substantia nigra (ventral

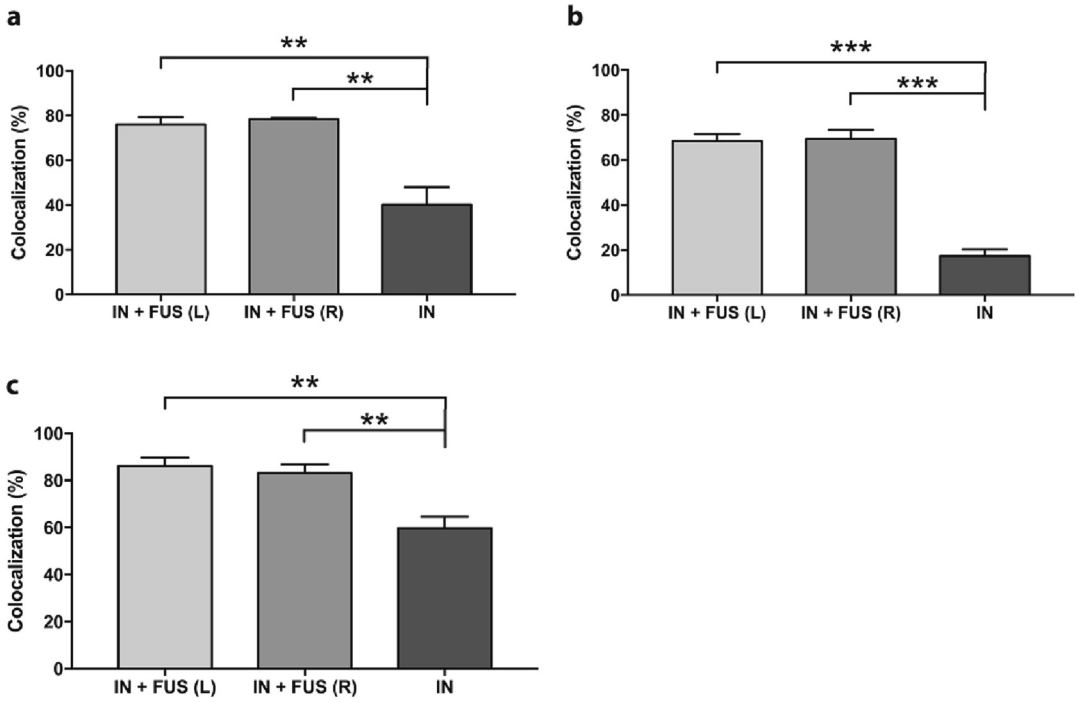

Fig. 9. Percentage of eGFP-positive cells that were located within 15 μm of neurons after intranasal administration of pUGG NPs, with or without FUS. Rats received the same dose (90 μg DNA) of pUGG NPs alone, or with application of FUS to the right forebrain and midbrain. The percentage of eGFP-positive cells that colocalized with (were within 15 μm) of NeuN-positive neurons in the forebrain (A) and midbrain (B), and the those that colocalized with TH-positive neurons in the midbrain (C) were quantified using Bioquant image analysis software. No significant difference was observed between the percent of eGFP-positive cells that were adjacent to NeuN-positive neurons on the sonicated side (L, left) vs the unsonicated side (R, right) of rats that received pUGG NPs intranasally with FUS. However, there was a significant increase in the percentage of eGFP-positive cells on both sides of FUS-treated rats vs unsonicated controls (one-way ANOVA, striatum: $P = 0.0024$, midbrain: $P < 0.0001$, Tukey's post-test: IN + FUS (left or right) vs IN alone, $^{*}P < 0.01$, $^{**}P < 0.001$). (C) No significant difference was observed between the percent of eGFP-positive cells that were adjacent to TH-positive neurons on the sonicated side (L, left) vs the unsonicated side (R, right) of rats that received pUGG NPs intranasally with FUS, although there was a significant increase in the percentage of eGFP-positive cells on both sides of FUS-treated rats vs unsonicated controls (one-way ANOVA, $P = 0.0025$, Tukey's post-test: IN + FUS (left or right) vs IN alone, $^{*}p < 0.01$).

midbrain) after intranasal administration of pUGG NPs (without FUS). Here, we observed that sonication at the level of the midbrain in rats that received the same dose of intranasal pUGG NPs increased the percentage of eGFP-positive cells that were found within 15 μm of a TH-positive dopaminergic neuron to over 80%, and did so in both the sonicated and unsonicated hemispheres (Fig. 9c). Since these changes were not confined to the sonicated hemisphere, it again appears that FUS induces changes in delivery and transfection by these NPs by a process which extends beyond the immediate sonicated areas.

4. Discussion

One of the main aims in this study was to demonstrate the feasibility of enhancing gene therapy efficacy by combining FUS and intranasal delivery. Here, we demonstrate a non-invasive and non-viral gene therapy approach that, when combined with FUS-facilitated BBB-opening, provides a means of spatially-targeting the gene therapy to particular brain regions. This technology overcomes some of the key limitations associated with conventional gene delivery to the brain, including bypassing the BBB, avoiding systemic exposure to the gene vector, and avoiding immunogenicity associated with viral vectors, while at the same time achieving enrichment of gene expression in desired brain regions. Microbubble-mediated FUS with intranasal administration of pUGG NPs resulted in an altered distribution of eGFP in the sonicated brain regions as well as the sonicated hemisphere, with higher levels of transgene expression on the sonicated side compared to the control side. This result was consistent with the hypothesis that FUS is likely to exert both localized "BBB disruption" as well as a generalized loosening of tight junctions between cells of the neurovascular unit at the sonication site, but also extending well beyond it. This widespread disruption of perivascular flow shifts the relative distribution of NPs to the sonicated areas while also facilitating NP transport, penetration and gene transfection throughout areas of the whole brain. Thus, while FUS is a localized treatment, its effects are not exclusively localized to the sonicated regions (which was reflected by the changes observed in regions beyond the immediate sonication site).

Since the nasal route exploits transport of substances by perivascular flow, and since FUS is postulated to cause widening of perivascular spaces, it is perhaps more likely that FUS enhances intranasal delivery to a greater degree than other routes such, as intravenous administration. Indeed, our results confirmed that microbubble-mediated FUS increased pUGG NP transgene expression to a greater extent after intranasal rather than intravenous administration of the same dose. The differing effectiveness of combining FUS with either intranasal or intravenous administration of the same dose of NPs could be due to several factors. First, *intranasal* administration resulted in transfection of perivascular cells throughout the whole brain, in addition to the increases in transfection at both the sonicated sites. On the other hand, *intravenous* administration of pUGG NPs with FUS resulted in only modest increases in transfection in the sonicated versus non-sonicated hemisphere (Fig. 2b) and no significant increase in whole brain eGFP expression above baseline in saline-treated controls (Fig. 2a). Secondly, the intravenous route involves a large dilution effect with only a small fraction of the dose reaching the brain via the blood. Even though the intranasal route is also inefficient, with traditionally <1% of the administered dose accessing the brain [41–43], it nevertheless targets the brain over the periphery, making it more capable of inducing transfection and transgene expression in the brain compared to the intravenous route.

Another main goal of this study was to identify the cell type(s) transfected after intranasal delivery of pUGG NPs with FUS application, and to assess whether the cellular transfection pattern was altered by FUS. In our previous studies involving intranasal administration of pUGG NPs alone (without FUS) we demonstrated that the majority of transfected cells were found immediately adjacent to and abluminal to capillaries. Based on their cellular morphology and location relative to RECA-1 positive capillary endothelial cells and GFAP-positive astrocytic endfeet enwrapping capillaries, the transfected cells were considered most likely to be pericytes [14] or other perivascular immune cells, such as macrophages or microglia. Since these perivascular cells share similar immunohistochemical markers, they are not distinguishable using specific antibody staining methods, and we did not attempt to identify them. In our current study, however, we confirmed that the transfected cells seen in the FUS-treated rats given intranasal pUGG NPs often expressed the cellular marker Iba1 even at sites distant from the sonication sites (see Sup Fig. 3). Thus, it is likely that a similar percentage of the transfected cells in our previous study [14], which did not involve FUS, were also Iba-1-positive.

We next examined whether FUS changed the pattern of cellular transfection. We initially hypothesized that with the application of FUS and consequent BBB opening, intranasally administered pUGG NPs would be able to leave perivascular spaces and penetrate deeper into the brain, enabling transfection of other cell types such as astrocytes and neurons. However, based on the series of double-label IHC studies that we carried out using different cellular markers, it was evident that the cells transfected at the sonication site were not positive for any of these markers. Accordingly, there was no colocalization of the transfected cells with either RECA-1 positive capillary endothelial cells, GFAP-positive astrocytes, NeuN-positive neurons, or TH-positive dopaminergic neurons. Instead, the cells transfected at the sonication sites appeared in dense clusters and were larger ameboid cells lacking processes and distributed throughout the parenchyma, not aligned along capillaries. Immunohistochemical analysis for eGFP and the cellular marker Iba1 confirmed that the majority of transfected cells at the sonication site are Iba1-positive, supporting their identification as microglia (and/or other perivascular immune cells that express Iba1).

The most plausible explanation for this clustering of transfected Iba1-positive is that activated microglia were recruited to the sonication site as a response to sonication (see Fig. 6). Kovacs et al. (2017) described a localized sterile inflammatory response to BBB disruption after application of low-intensity FUS with microbubbles, and correlated this with extravasation of albumin, increases in various pro-inflammatory cytokines, and activation of microglia [39]. This raises the question whether microglia are being transfected by pUGG NPs because they are migrating to the sites of BBB opening due to this inflammatory response to FUS. Reactive microglia are more capable of phagocytosis [39], possibly leading to their uptake of pUGG NPs (that had penetrated the parenchyma at those sites) and subsequent transfection. A remote possibility is that microglia may be migrating to these sites by phagocytic attraction to the NPs themselves. This seems unlikely based on results of direct intracranial injection of other identically formulated GDNF DNA NPs. For example, Yurek et al. (2009) demonstrated transfection of both GFAP-positive astrocytes and NeuN-positive neurons, but no microglial recruitment or transfection [44]. In fact, in our current study, control rats that received FUS with circulating microbubbles (using the same sonication parameters) but no intranasal NPs also showed evidence of microglial activation/recruitment at the sonication sites, but not at distant non-sonicated sites. This negates the possibility that the microglia may be migrating to sonication sites due to the presence of the NPs. This result is in line with work carried out by others that demonstrate that FUS causes transient activation of microglia and astrocytes [38,39] and indicates that microglia recruitment occurs as a result of FUS and not the introduction of the DNA NPs into the brain parenchyma.

Since FUS with microbubbles results in transfection of microglia after intranasal administration of pUGG NPs, the implications of microglial production of GDNF in the brain will be of critical importance. The most important unresolved question is whether recruitment of activated microglia to target sites in Parkinson's disease will cause toxicities due to their release of pro-inflammatory cytokines in these vulnerable brain regions. It has been suggested that the microglial activation due to FUS is transient and resolves within a week or two after treatments [38,39]. GDNF co-expression by these transfected microglia may help to counteract any tissue damage. In this regard, it will also be of importance to examine the localization of transfected microglia in the brain past the one-week time point in this study. In our previous studies, we demonstrated that transgene expression by perivascular cells following intranasal delivery of pUGG NPs persists for at least 6 months. Whether combining FUS with intranasal pUGG NPs will change the time-course of transgene expression remains to be seen.

Although the expression of GDNF by cells other than glia has not been widely studied, there are reports that microglia do express both the GDNF receptor, GFRα, as well as the RET tyrosine kinase co-receptor [45,46]. In vitro studies of the effect of GDNF on primary microglia cultures have demonstrated that GDNF has little or no effect on microglial production of the pro-inflammatory cytokines, TNF-α and IL-1β, although it does increase ICAM-1 mRNA, integrin-α5 expression, SOD enzymatic activity, as well as phagocytic uptake [47]. Thus, GDNF may play a role in regulating microglial activity in the brain, by enhancing their anti-oxidant and phagocytic properties, and possibly contributing to the neuroprotective effects of GDNF in vivo.

We further demonstrated that FUS redistributed the expression of pUGG NPs, and it improved their penetration into the brain parenchyma. In previous studies, the majority of eGFP-positive cells after intranasal administration of pUGG NPs were located immediately adjacent to and abluminal to blood vessels throughout the brain, with <40% of eGFP-positive cells located in close proximity to NeuN-positive neurons in the forebrain and midbrain, and <60% located within 15 μm of TH-positive neurons in the SN. However, application of FUS with circulating microbubbles resulted in transfection of a higher percentage of cells that are located in close proximity to neurons in both the striatum and midbrain, the regions of interest in Parkinson's disease. These results suggest that FUS with microbubbles does increase the penetration of these plasmid DNA NPs into the brain parenchyma (in both the sonicated and unsonicated hemispheres) after intranasal administration. However, they raise the question of why this change was not confined to the sonicated brain region and/or hemisphere. As alluded to above, we speculate that application of FUS might alter the perivascular flow parameters in the whole brain, thus influencing the bulk-flow of intranasally delivered substances throughout the brain. This possibility is consistent with studies by Hersh et al. (2016), which demonstrated that application of pulsed ultrasound can expand extracellular and perivascular spaces in the brain, as well as increase the diffusion rate of various-sized nanoparticles (100 nm, 200 nm, and 500 nm) [48]. It stands to reason that changes in the diameter of microvessels as a result of the FUS-induced oscillation of microbubbles may affect the overall distribution of intranasally administered agents that are traveling in perivascular spaces throughout the brain.

5. Conclusions

These studies provide the first evidence that ultrasound can be used to enhance the intranasal delivery of plasmid DNA nanoparticles to the rodent brain, in this case, the forebrain and midbrain, by recruitment and transfection of microglia. By successfully combining three unique approaches (non-viral gene therapy, intranasal delivery, and focused ultrasound), this work provides proof-of-concept for a long-term, completely non-invasive means of targeting a gene therapy to the brain whilst avoiding peripheral side effects. This approach has potential for improved non-invasive gene transfer for Parkinson's disease and other CNS disorders, provided toxicology studies determine no

significant brain injury related to FUS application. Refining FUS parameters to achieve a safe means of enhancing intranasal delivery of these DNA NPs to the brain is the next step in realizing this potential.

Funding

This research was supported by the Focused Ultrasound Surgery Foundation, Research Awards Program, High Risk Track.

CRediT authorship contribution statement

Amirah E.-E. Aly: Conceptualization, Formal analysis, Investigation, Methodology, Visualization, Writing – original draft, Writing – review & editing. **Tao Sun:** Formal analysis, Investigation, Methodology, Writing – review & editing. **Yongzhi Zhang:** Investigation, Methodology. **Zejun Li:** Investigation. **Margee Kyada:** Investigation. **Qingxi Ma:** Investigation. **Linas Padegimas:** Resources. **Ozge Sesenoglu-Laird:** Resources. **Mark J. Cooper:** Resources, Writing – review & editing. **Nathan J. McDannold:** Conceptualization, Funding acquisition, Supervision, Writing – review & editing. **Barbara L. Waszczak:** Conceptualization, Funding acquisition, Supervision, Writing – review & editing.

Data availability

Data will be made available on request.

Appendix A. Supplementary data

Supplementary data to this article can be found online at https://doi.org/10.1016/j.jconrel.2023.04.041.

References

[1] N.K. Patel, M. Bunnage, P. Plaha, C.N. Svendsen, P. Heywood, S.S. Gill, Intraputamenal infusion of glial cell line-derived neurotrophic factor in PD: a two-year outcome study, Annals of Neurology 57 (2005) 298–302, https://doi.org/10.1002/ana.20374.

[2] W.J. Marks, J.L. Ostrem, L. Verhagen, P.A. Starr, P.S. Larson, R.A. Bakay, R. Taylor, D.A. Cahn-Weiner, A.J. Stoessl, C.W. Olanow, R.T. Bartus, Safety and tolerability of intraputaminal delivery of CERE-120 (adeno-associated virus serotype 2–neurturin) to patients with idiopathic Parkinson's disease: an open-label, phase I trial, Lancet Neurol. 7 (2008) 400–408, https://doi.org/10.1016/S1474-4422(08)70065-6.

[3] R.T. Bartus, T.L. Baumann, J. Siffert, C.D. Herzog, R. Alterman, N. Boulis, D. A. Turner, M. Stacy, A.E. Lang, A.M. Lozano, C.W. Olanow, Safety/feasibility of targeting the substantia nigra with AAV2-neurturin in Parkinson patients, Neurology 80 (2013) 1698–1701, https://doi.org/10.1212/wnl.0b013e3182904faa.

[4] S. Love, P. Plaha, N.K. Patel, G.R. Hotton, D.J. Brooks, S.S. Gill, Glial cell line–derived neurotrophic factor induces neuronal sprouting in human brain, Nat. Med. 11 (2005) 703–704, https://doi.org/10.1038/nm0705-703.

[5] J.T. Slevin, G.A. Gerhardt, C.D. Smith, D.M. Gash, R. Kryscio, B. Young, Improvement of bilateral motor functions in patients with Parkinson disease through the unilateral intraputaminal infusion of glial cell line—derived neurotrophic factor, J. Neurosurg. 102 (2005) 216–222, https://doi.org/10.3171/jns.2005.102.2.0216.

[6] J.G. Nutt, K.J. Burchiel, C.L. Comella, J. Jankovic, A.E. Lang, E.R. Laws, A. M. Lozano, R.D. Penn, R.K. Simpson, M. Stacy, G.F. Wooten, the I.G.S. Group*, Randomized, double-blind trial of glial cell line-derived neurotrophic factor (GDNF) in PD, Neurology 60 (2003) 69–73, https://doi.org/10.1212/wnl.60.1.69.

[7] S.S. Gill, N.K. Patel, G.R. Hotton, K. O'Sullivan, R. McCarter, M. Bunnage, D. J. Brooks, C.N. Svendsen, P. Heywood, Direct brain infusion of glial cell line–derived neurotrophic factor in Parkinson disease, Nat. Med. 9 (2003) 589–595, https://doi.org/10.1038/nm850.

[8] A.E. Lang, S. Gill, N.K. Patel, A. Lozano, J.G. Nutt, R. Penn, D.J. Brooks, G. Hotton, E. Moro, P. Heywood, M.A. Brodsky, K. Burchiel, P. Kelly, A. Dalvi, B. Scott, M. Stacy, D. Turner, V.G.F. Wooten, W.J. Elias, E.R. Laws, V. Dhawan, A.J. Stoessl, J. Matcham, R.J. Coffey, M. Traub, Randomized controlled trial of intraputamenal glial cell line–derived neurotrophic factor infusion in Parkinson disease, Ann. Neurol. 59 (2006) 459–466, https://doi.org/10.1002/ana.20737.

[9] S.V. Dhuria, L.R. Hanson, W.H. Frey, Intranasal delivery to the central nervous system: mechanisms and experimental considerations, J. Pharm. Sci. 99 (2010) 1654–1673, https://doi.org/10.1002/jps.21924.

[10] G. Liu, D. Li, M.K. Pasumarthy, T.H. Kowalczyk, C.R. Gedeon, S.L. Hyatt, J. M. Payne, T.J. Miller, P. Brunovskis, T.L. Fink, O. Muhammad, R.C. Moen, R. W. Hanson, M.J. Cooper, Nanoparticles of compacted DNA transfect postmitotic cells, J. Biol. Chem. 278 (2003) 32578–32586, https://doi.org/10.1074/jbc.M305776200.

[11] A.-G. Ziady, C.R. Gedeon, T. Miller, W. Quan, J.M. Payne, S.L. Hyatt, T.L. Fink, O. Muhammad, S. Oette, T. Kowalczyk, M.K. Pasumarthy, R.C. Moen, M.J. Cooper, P.B. Davis, Transfection of airway epithelium by stable PEGylated poly-l-lysine DNA nanoparticles in vivo, Mol. Ther. 8 (2003) 936–947, https://doi.org/10.1016/j.ymthe.2003.07.007.

[12] A.M. Fletcher, T.H. Kowalczyk, L. Padegimas, M.J. Cooper, D.M. Yurek, Transgene expression in the striatum following intracerebral injections of DNA nanoparticles encoding for human glial cell line-derived neurotrophic factor, Neuroscience 194 (2011) 220–226, https://doi.org/10.1016/j.neuroscience.2011.07.072.

[13] A.E.-E. Aly, B.T. Harmon, L. Padegimas, O. Sesenoglu-Laird, M.J. Cooper, B. L. Waszczak, Intranasal delivery of pGDNF DNA nanoparticles provides neuroprotection in the rat 6-hydroxydopamine model of Parkinson's disease, Mol. Neurobiol. 56 (2019) 688–701, https://doi.org/10.1007/s12035-018-1109-6.

[14] A.E.-E. Aly, B. Harmon, L. Padegimas, O. Sesenoglu-Laird, M.J. Cooper, D. M. Yurek, B.L. Waszczak, Intranasal delivery of hGDNF plasmid DNA nanoparticles results in long-term and widespread transfection of perivascular cells in rat brain, Nanomed. Nanotechnol. Biol. Med. 16 (2019) 20–33, https://doi.org/10.1016/j.nano.2018.11.006.

[15] K. Hynynen, N. McDannold, N. Vykhodtseva, F.A. Jolesz, Noninvasive MR imaging–guided focal opening of the blood-brain barrier in rabbits, Radiology 220 (2001) 640–646, https://doi.org/10.1148/radiol.2202001804.

[16] K. Hynynen, N. McDannold, N.A. Sheikov, F.A. Jolesz, N. Vykhodtseva, Local and reversible blood–brain barrier disruption by noninvasive focused ultrasound at frequencies suitable for trans-skull sonications, NeuroImage 24 (2005) 12–20, https://doi.org/10.1016/j.neuroimage.2004.06.046.

[17] X. Shang, P. Wang, Y. Liu, Z. Zhang, Y. Xue, Mechanism of low-frequency ultrasound in opening blood–tumor barrier by tight junction, J. Mol. Neurosci. 43 (2011) 364–369, https://doi.org/10.1007/s12031-010-9451-9.

[18] N. Sheikov, N. McDannold, F. Jolesz, Y.-Z. Zhang, K. Tam, K. Hynynen, Brain arterioles show more active vesicular transport of blood-borne tracer molecules than capillaries and venules after focused ultrasound-evoked opening of the blood-brain barrier, Ultrasound Med. Biol. 32 (2006) 1399–1409, https://doi.org/10.1016/j.ultrasmedbio.2006.05.015.

[19] N. Sheikov, N. McDannold, N. Vykhodtseva, F. Jolesz, K. Hynynen, Cellular mechanisms of the blood-brain barrier opening induced by ultrasound in presence of microbubbles, Ultrasound Med. Biol. 30 (2004) 979–989, https://doi.org/10.1016/j.ultrasmedbio.2004.04.010.

[20] M. Kinoshita, N. McDannold, F.A. Jolesz, K. Hynynen, Noninvasive localized delivery of Herceptin to the mouse brain by MRI-guided focused ultrasound-induced blood–brain barrier disruption, Proc. Natl. Acad. Sci. 103 (2006) 11719–11723, https://doi.org/10.1073/pnas.0604318103.

[21] L.H. Treat, N. McDannold, N. Vykhodtseva, Y. Zhang, K. Tam, K. Hynynen, Targeted delivery of doxorubicin to the rat brain at therapeutic levels using MRI-guided focused ultrasound, Int. J. Cancer 121 (2007) 901–907, https://doi.org/10.1002/ijc.22732.

[22] E.-J. Park, Y.-Z. Zhang, N. Vykhodtseva, N. McDannold, Ultrasound-mediated blood-brain/blood-tumor barrier disruption improves outcomes with trastuzumab in a breast cancer brain metastasis model, J. Control. Release 163 (2012) 277–284, https://doi.org/10.1016/j.jconrel.2012.09.007.

[23] M. Aryal, N. Vykhodtseva, Y.-Z. Zhang, J. Park, N. McDannold, Multiple treatments with liposomal doxorubicin and ultrasound-induced disruption of blood–tumor and blood–brain barriers improve outcomes in a rat glioma model, J. Control. Release 169 (2013) 103–111, https://doi.org/10.1016/j.jconrel.2013.04.007.

[24] C.A. Nosrat, A. Tomac, B.J. Hoffer, L. Olson, Cellular and developmental patterns of expression of ret and glial cell line-derived neurotrophic factor receptor alpha mRNAs, Exp. Brain Res. 115 (1997) 410–422, https://doi.org/10.1007/pl00005711.

[25] D. Ye, X. Zhang, Y. Yue, R. Raliya, P. Biswas, S. Taylor, Y. Tai, J.B. Rubin, Y. Liu, H. Chen, Focused ultrasound combined with microbubble-mediated intranasal delivery of gold nanoclusters to the brain, J. Control. Release 286 (2018) 145–153, https://doi.org/10.1016/j.jconrel.2018.07.020.

[26] H. Chen, C.C. Chen, C. Acosta, S.-Y. Wu, T. Sun, E.E. Konofagou, A new brain drug delivery strategy: focused ultrasound-enhanced intranasal drug delivery, PLoS One 9 (2014), e108880, https://doi.org/10.1371/journal.pone.0108880.

[27] H. Chen, G.Z.X. Yang, H. Getachew, C. Acosta, C. Sierra Sánchez, E.E. Konofagou, Focused ultrasound-enhanced intranasal brain delivery of brain-derived neurotrophic factor, Sci. Rep. 6 (2016) 28599, https://doi.org/10.1038/srep28599.

[28] B.T. Harmon, A.E. Aly, L. Padegimas, O. Sesenoglu-Laird, M.J. Cooper, B. L. Waszczak, Intranasal administration of plasmid DNA nanoparticles yields successful transfection and expression of a reporter protein in rat brain, Gene Ther. 21 (2014) 514–521, https://doi.org/10.1038/gt.2014.28.

[29] T.L. Fink, P.J. Klepcyk, S.M. Oette, C.R. Gedeon, S.L. Hyatt, T.H. Kowalczyk, R. C. Moen, M.J. Cooper, Plasmid size up to 20 kbp does not limit effective in vivo lung gene transfer using compacted DNA nanoparticles, Gene Ther. 13 (2006) 1048–1051, https://doi.org/10.1038/sj.gt.3302761.

[30] T. Sun, J.T. Sutton, C. Power, Y. Zhang, E.L. Miller, N.J. McDannold, Transcranial cavitation-mediated ultrasound therapy at sub-MHz frequency via temporal interference modulation, Appl. Phys. Lett. 111 (16) (2023), https://doi.org/10.1063/1.5000896.

[31] T. Sun, Y. Zhang, C. Power, P.M. Alexander, J.T. Sutton, M. Aryal, N. Vykhodtseva, E.L. Miller, N.J. McDannold, Closed-loop control of targeted ultrasound drug delivery across the blood–brain/tumor barriers in a rat glioma model, Proc. Natl.

Acad. Sci. 114 (2017) E10281–E10290, https://doi.org/10.1073/pnas.1713328114.
[32] T. Ilovitsh, A. Ilovitsh, J. Foiret, C.F. Caskey, J. Kusunose, B.Z. Fite, H. Zhang, L. M. Mahakian, S. Tam, K. Butts-Pauly, S. Qin, K.W. Ferrara, Enhanced microbubble contrast agent oscillation following 250 kHz insonation, Scientific Reports 8 (2018), https://doi.org/10.1038/s41598-018-34494-5.
[33] T.S. Bender, M.M. Migliore, R.B. Campbell, S. John Gatley, B.L. Waszczak, Intranasal administration of glial-derived neurotrophic factor (GDNF) rapidly and significantly increases whole-brain GDNF level in rats, Neuroscience 303 (2015) 569–576, https://doi.org/10.1016/j.neuroscience.2015.07.016.
[34] I. Özen, T. Deierborg, K. Miharada, T. Padel, E. Englund, G. Genové, G. Paul, Brain pericytes acquire a microglial phenotype after stroke, Acta Neuropathol. (Berl.) 128 (2014) 381–396, https://doi.org/10.1007/s00401-014-1295-x.
[35] G.J. Guillemin, B.J. Brew, Microglia, macrophages, perivascular macrophages, and pericytes: a review of function and identification, J. Leukoc. Biol. 75 (2004) 388–397.
[36] B. Hutter-Schmid, C. Humpel, Primary mouse brain pericytes isolated from transgenic Alzheimer mice spontaneously differentiate into a CD11b+ microglial-like cell type in vitro, Exp. Gerontol. 112 (2018) 30–37, https://doi.org/10.1016/j.exger.2018.08.003.
[37] R. Sakuma, M. Kawahara, A. Nakano-Doi, A. Takahashi, Y. Tanaka, A. Narita, S. Kuwahara-Otani, T. Hayakawa, H. Yagi, T. Matsuyama, T. Nakagomi, Brain pericytes serve as microglia-generating multipotent vascular stem cells following ischemic stroke, J. Neuroinflammation 13 (57) (2016), https://doi.org/10.1186/s12974-016-0523-9.
[38] J.F. Jordão, E. Thévenot, K. Markham-Coultes, T. Scarcelli, Y.Q. Weng, K. Xhima, M. O'Reilly, Y. Huang, J. McLaurin, K. Hynynen, I. Aubert, Amyloid-β plaque reduction, endogenous antibody delivery and glial activation by brain-targeted, transcranial focused ultrasound, Exp Neurol. 248 (2013) 16–29, https://doi.org/10.1016/j.expneurol.2013.05.008.
[39] Z.I. Kovacs, S. Kim, N. Jikaria, F. Qureshi, B. Milo, B.K. Lewis, M. Bresler, S. R. Burks, J.A. Frank, Disrupting the blood–brain barrier by focused ultrasound induces sterile inflammation, Proc. Natl. Acad. Sci. 114 (2017) E75–E84, https://doi.org/10.1073/pnas.1614777114.
[40] D.J. Wolak, R.G. Thorne, Diffusion of macromolecules in the brain: implications for drug delivery, Mol. Pharm. 10 (2013) 1492–1504, https://doi.org/10.1021/mp300495e.
[41] R.G. Thorne, W.H. Frey, Delivery of neurotrophic factors to the central nervous system, Clin. Pharmacokinet. 40 (2001) 907–946, https://doi.org/10.2165/00003088-200140120-00003.
[42] M.M. Migliore, T.K. Vyas, R.B. Campbell, M.M. Amiji, B.L. Waszczak, Brain delivery of proteins by the intranasal route of administration: a comparison of cationic liposomes versus aqueous solution formulations, J. Pharm. Sci. 99 (2010) 1745–1761, https://doi.org/10.1002/jps.21939.
[43] R.G. Thorne, L.R. Hanson, T.M. Ross, D. Tung, W.H. Frey, Delivery of interferon-β to the monkey nervous system following intranasal administration, Neuroscience 152 (2008) 785–797, https://doi.org/10.1016/j.neuroscience.2008.01.013.
[44] D.M. Yurek, A.M. Fletcher, G.M. Smith, K.B. Seroogy, A.G. Ziady, J. Molter, T. H. Kowalczyk, L. Padegimas, M.J. Cooper, Long-term transgene expression in the central nervous system using DNA nanoparticles, Mol. Ther. 17 (2009) 641–650, https://doi.org/10.1038/mt.2009.2.
[45] D.G. Walker, T.G. Beach, R. Xu, J. Lile, K.D. Beck, E.G. McGeer, P.L. McGeer, Expression of the proto-oncogene ret, a component of the GDNF receptor complex, persists in human substantia nigra neurons in Parkinson's disease, Brain Res. 792 (1998) 207–217, https://doi.org/10.1016/s0006-8993(98)00131-0.
[46] S. Honda, K. Nakajima, Y. Nakamura, Y. Imai, S. Kohsaka, Rat primary cultured microglia express glial cell line-derived neurotrophic factor receptors, Neurosci. Lett. 275 (1999) 203–206, https://doi.org/10.1016/S0304-3940(99)00769-7.
[47] Y.-P. Chang, K.-M. Fang, T.-I. Lee, S.-F. Tzeng, Regulation of microglial activities by glial cell line derived neurotrophic factor, J. Cell. Biochem. 97 (2006) 501–511, https://doi.org/10.1002/jcb.20646.
[48] D.S. Hersh, B.A. Nguyen, J.G. Dancy, A.R. Adapa, J.A. Winkles, G.F. Woodworth, A.J. Kim, V. Frenkel, Pulsed ultrasound expands the extracellular and perivascular spaces of the brain, Brain Res. 1646 (2016) 543–550, https://doi.org/10.1016/j.brainres.2016.06.040.